Ring Polymer Molecular Dynamics Calculations of Thermal Rate Constants for the O([superscript 3]P) + CH[subscript 4] → OH + CH[subscript 3] Reaction: Contributions of Quantum Effects

Citation: Li, Yongle, Yury V. Suleimanov, Minghui Yang, William H. Green, and Hua Guo. "Ring Polymer Molecular Dynamics Calculations of Thermal Rate Constants for the O([superscript 3]P) + CH[subscript 4] → OH + CH[subscript 3] Reaction: Contributions of Quantum Effects." The Journal of Physical Chemistry Letters 4, no. 1 (January 3, 2013): 48–52.

As Published: http://dx.doi.org/10.1021/jz3019513

Publisher: American Chemical Society (ACS)

Persistent URL: http://hdl.handle.net/1721.1/92367

Version: Author's final manuscript: final author's manuscript post peer review, without publisher's formatting or copy editing

Submitted to JPCL, 11/26/2012

Ring polymer molecular dynamics calculations of thermal rate constants for the $O(^3P) + CH_4 \rightarrow OH + CH_3$ reaction: Contributions of quantum effects

Yongle Li,[1,#] Yury V. Suleymanov,[2,#,] Minghui Yang,[3] William H. Green,[2] and Hua Guo[1,*]*

[1]*Department of Chemistry and Chemical Biology, University of New Mexico, Albuquerque, NM 87131, USA*

[2]*Department of Chemical Engineering, Massachusetts Institute of Technology, Cambridge, MA 02139, USA*

[3]*Wuhan Center for Magnetic Resonance, State Key Laboratory of Magnetic Resonance and Atomic and Molecular Physics, Wuhan Institute of Physics and Mathematics, Chinese Academy of Sciences, Wuhan 430071, China*

#: Equally contributed to this work.

*: Corresponding authors. Emails: ysuleyma@mit.edu, hguo@unm.edu

Abstract

The thermal rate constant of the $O(^3P) + CH_4 \rightarrow OH + CH_3$ reaction is investigated with ring polymer molecular dynamics on a full-dimensional potential energy surface. Good agreement with experimental and full-dimensional quantum multi-configuration time-dependent Hartree results between 300 and 1500 K was obtained. It is shown that quantum effects, e.g. tunneling and zero-point energy, can be effectively and efficiently included in this path-integral based approach implemented with classical trajectories. Convergence with respect to the number of beads is rapid, suggesting wide applicability for other reactions involving polyatomic molecules.

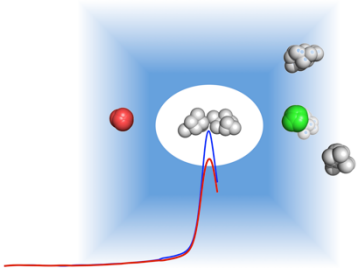

TOC graphic

Key words: reaction rates, tunneling, zero-point energy, path integral, combustion

Accurate determination of rate constants of gas phase bimolecular reactions is of central importance in modeling kinetics of atmospheric (*1*) and combustion systems.(*2*) While accurate rate constants can often be measured,(*3*) theoretical approaches are complementary with many additional benefits. For instance, experimental measurements of certain reactions might not always be possible and/or reliable at the temperatures of interest. In addition, an accurate determination of the rate constant provides insights into the dynamics and mechanism of the reaction, and offers a stringent test of the underlining potential energy surface, particularly in the transition-state region.

Many bimolecular reactions, particularly those in combustion, involve the transfer of a hydrogen atom. As a result, these reactions are affected by many quantum effects, such as zero-point energy (ZPE) and tunneling, particularly at low temperatures. Ideally, the rate constant of such a reaction should be determined using an exact quantum mechanical method on an accurate potential energy surface.(*4-5*) However, these methods are only amenable to reactions involving a few atoms because of their steep scaling laws with the number of degrees of freedom, even when the most efficient variant, namely the multi-configuration time-dependent Hartree (MCTDH) method, is used.(*6*)

Several approximate methods have thus been developed to take into consideration of these quantum effects within the framework of transition-state theory.(*7*) While ZPE can often be included in the theoretical treatment with relative ease, tunneling remains a difficult issue. The approximate models for treating tunneling over the reaction barrier include not only the well-established small-curvature tunneling (SCT), large-curvature tunneling (LCT), and the microcanonical optimized multidimensional tunneling (μOMT) methods,(*7*) but also the recently implemented (*8*) semi-classical transition-state theory.(*9-10*) However, these semi-classical

models are often unreliable in the deep tunneling regime due to the multidimensional nature of quantum tunneling.

A different approach is based the so-called ring polymer molecular dynamics (RPMD) method,(*11*) which is an approximate quantum mechanical method based on the isomorphism between the statistical properties of a quantum system and a fictitious ring polymer consisting of a number of classical beads connected with harmonic potentials.(*12*) Its path integral nature allows the inclusion of quantum effects, while its classical implementation endows it with favorable scaling laws. Recently, it has been formulated by Manolopoulos and coworkers to compute rate constants for chemical reactions.(*13-14*) Specifically for gas phase bimolecular reactions, the Bennett-Chandler factorization (*15-16*) was adapted for computing the RPMD rate constants:(*17-18*)

$$k_{RPMD}(T) = f(T)\kappa(\xi^{\neq})k_{QTST}(T,\xi^{\neq}), \qquad (1)$$

where $k_{QTST}(T,\xi^{\neq})$ is the rate constant computed from the centroid-density quantum transition-state theory at $\xi^{\neq}$, namely the peak position along the reaction coordinate ξ. This static component is obtained from the potential of mean force (PMF) along the reaction coordinate, which is calculated by umbrella integration (*19*) of the RPMD distributions in windows along the reaction coordinate biased with harmonic potentials. On the other hand, $\kappa(\xi^{\neq})$ is the long-time ($t \to \infty$) limit of the ring polymer transmission coefficient, which represents the dynamic correction. It can be determined from recrossing trajectories with their initial centroids placed at the transition state. Finally, $f(T)$ is the electronic degeneracy factor. For the title reaction, it includes the electronic and spin-orbit partition functions with the following form:(*20-21*)

$$f(T) = \frac{3k(1^3A) + 3k(2^3A)}{5 + 3e^{-E(^3P_1)/RT} + e^{-E(^3P_0)/RT}}, \qquad (2)$$

where $E(^3P_1)$ and $E(^3P_0)$ are the energies of the upper spin-orbit levels of O(^3P) relative to that of $^3P_2$, with the values 158.29 and 226.99 cm^{-1}, respectively. In addition, the numerator in Eq. (2) was approximated by $6k(1^3A)$ as both triplet Jahn-Teller states have similar transition states, but only one (1^3A) was included in the calculation.

The RPMD approach has a number of distinct advantages. First, it gives the exact rate constant in the high temperature limit as the ring polymer collapses to a single classical bead. Second, it treats all degrees of freedom on an equal footing and as a result is truly full dimensional. In addition, it does not depend on the choice of the dividing surfaces, which is important for large systems where the optimum dividing surface is hard to locate. The PMF approach is also numerically advantageous for large systems since no partition function needs to be explicitly calculated. Finally, since it is implemented with classical trajectories, it scales much more slowly with the degrees of freedom than any quantum mechanical methods and is thus applicable for much larger systems. In fact, an RPMD calculation is roughly *n* times more expensive than the conventional classical trajectory method, where *n* is the number of beads in the ring polymer. The RPMD approach has recently been applied to several bimolecular reactions with impressive success.(*17-18, 22-23*) In particular, it performed quite well in the deep tunneling regime, a surprising phenomenon explained by the recent analysis of Richardson and Althorpe.(*24*)

In this Letter, we report the application of RPMD to a hydrogen abstraction reaction involving six atoms. The O(^{3}P) + CH_4 → OH + CH_3 reaction represents an important initial step

in hydrocarbon combustion.(*25*) Technically, this reaction differs from $H + CH_4 \rightarrow H_2 + CH_3$, which has recently been studied using RPMD,(*18*) in that the small skew angle for this "heavy-light-heavy" system poses a significant challenge for characterizing the tunneling and barrier recrossing effects.(*26*) Several full-dimensional potential energy surfaces (PESs) of this important combustion reaction have been developed,(*20, 27*) including a recent one based on a large number of *ab initio* points.(*28*) The thermal rate constant has been determined using canonical variational transition-state theory with tunneling corrections,(*20-21, 27*) quasi-classical trajectory (QCT),(*29-30*) reduced-dimensional quantum dynamics (QD) methods,(*31-34*) as well a full-dimensional MCTDH method.(*35*) In this work, we choose to use the analytical PES of Espinosa-García and García-Bernáldez,(*27*) because it has been used in the earlier seven-dimensional (7D) QD study of Yang *et al*.(*34*), the MCTDH work of Huarte-Larrañaga and Manthe,(*35*) and transition-state theory calculations.(*27*) Two important features of this PES are noteworthy: It is symmetric with respect to the permutation of the four hydrogen atoms and the first energy derivatives are analytical, which allows accurate and efficient propagation of classical trajectories. We will report in a future work the RPMD rate constants on the more recent *ab initio* based PES of Czakó and Bowman.(*28*)

The RPMD calculations were performed using the RPMDrate code.(*36*) The RPMD procedure for calculating rate constants of bimolecular reactions has been discussed in details in Ref. (*36*), so only the specifics are given here. Different from previous studies,(*17-18, 22*) the PMF was calculated with different window sizes. In the relatively flat region, namely the entrance channel (ξ<0.75), larger windows ($d\xi$=0.08) with a small harmonic bias force constant k=0.34 (T/K) eV were used. On the other hand, the transition-state region, where the free energy changes drastically with the reaction coordinate, was covered with smaller windows

with a larger bias force constant ($d\xi$ =0.01 and k=2.72 (T/K) eV). In each window, the sampling was performed for 5 ns, and longer propagation does not change the results. In calculating the transmission coefficient, 100,000 unconstrained child trajectories were propagated for 0.05 ps with initial conditions sampled from a mother trajectory with its centroid constrained at the transition-state geometry. All calculations were performed with a time step of 0.1 fs.

Figure 1 displays the PMFs at 600 K obtained with one and eight beads. It is clear that the PMFs are reasonably flat in the entrance channel, and rise quickly when the system approaches the transition state. The RPMD activation free energy ($\Delta G^{\neq}$) is 15.7 kcal/mol, which is significantly lower than the classical free-energy barrier of 18.2 kcal/mol obtained with a single bead. This difference stems apparently from the quantum effects, including both zero-point energy and tunneling. A similar lowering of the activation free energy was observed at other temperatures.

In this work, we consider five different temperatures, 300, 400, 600, 900, and 1500 K. To establish convergence with respect to the number of beads, the RPMD simulations were first carried out with one bead per atom, which represents the classical limit. Larger numbers, namely 4, 8, 16, and 32, were used until the rate constant converges. The rate constants obtained with different beads at different temperatures are collected in Fig. 2. The classical rate constants form a perfect Arrhenius line in the log$k$ vs 1/T plot. As temperature decreases, quantum mechanical effects become important and a larger number of beads is needed to converge the results.

It is well established that the number of ring polymer beads for converged path integral calculations should satisfy the following relationship:(*37*)

$$n > n_{\min} \equiv \frac{\hbar \omega_{\max}}{k_B T}, \qquad (3)$$

where $\omega_{\max}$ is the largest frequency of the system. For the title reaction, $\omega_{\max}$ corresponds to the OH vibration in the product region and is equal to 3725 cm^{-1}.(*27*) Interestingly, we found that our results converge quickly with only a small number of beads which satisfies the criterion in Eq. (3). At the lowest temperature studied here (300 K), for example, 32 beads were sufficient to capture most of the quantum mechanical contributions while $n_{\min} \sim 18$. At the highest temperature (1500 K), on the other hand, four beads were sufficient with $n_{\min} \sim 4$, underscoring the fact that quantum mechanical effects become less important at high temperatures.

It is also interesting to note that the quantum mechanical effects are captured mostly by the first few beads. Indeed, the rate constant at 300 K increases approximately 122 times when the number of beads increases from 1 to 4, where it only changes about three times from 4 to 32 beads. This is quite important as it shows that the RPMD approach should scale quite well with the size of the system.

In Table I, additional information of the RPMD rate constants is listed. As expected, the activation free-energy ($\Delta G^{\neq}$) increases monotonically with the temperature, underscoring the contribution from tunneling at low temperatures. Interestingly, the position of the free-energy barrier ($\xi^{\neq}$) is slightly less than 1.0, which indicates that initial dividing surface defined in terms of the breaking and forming bond lengths (*36*) is not optimum. However, barrier recrossing at $\xi^{\neq}$ is still quite prevalent at all temperatures as evidenced by non-unity transmission coefficients. Interestingly, κ decreases with decreasing temperature, a phenomenon observed in previous RPMD studies.(*17-18*)

The RPMD rate constants are compared in Fig. 3 and Table I with both experimental data and previous theoretical results. It is quite interesting to note that the RPMD results agree almost perfectly with the MCTDH values at all temperatures. Although it is expected that the two different implementations of the same quantum dynamical theory should yield similar results, the perfect agreement between the two might be fortuitous due to error cancelation since both approaches contain some approximations. On the other hand, it is evident that the 7D QD results are significantly smaller. Since contributions from the lowest few vibrational states were included in the 7D QD rate constant, the difference may be attributed to the excited rotational states of the methane reactant, which were not included in the scattering calculations.

From Fig. 3 and Table I, we note that the agreement between the RPMD and the canonical unified statistical model with the μOMT tunneling correction (CUS-μOMT) of Espinosa-García and García-Bernáldez (*27*) is reasonably good. Quantitatively, however, the CUS-μOMT rate constants are higher than both the MCTDH and RPMD counterparts except for 1500 K where they are quite similar. There are several possible reasons for the deviations. At high temperatures, for example, recrossing in this heavy-light-heavy system may be prevalent, which is only partially taken into account in the variational transition-state theory. However, the good agreement between the RPMD/MCTDH and CUS-μOMT results at 1500 K seems to suggest that recrossing is a minor problem. Below the crossover temperature (356 K for the title reaction), on the other hand, the deep tunneling nature of the reaction rules out an accurate account of the tunneling contribution by a semi-classical model. Between the two limits, the overestimation of the rate constants by the CUS-μOMT model is probably due to a combination of errors in describing barrier recrossing and tunneling.

From the same figure, it is clear that the RPMD results are in reasonably good agreement with the experimental rate constants.(*3, 38*) While reproducing the curvature of the temperature dependence of the rate constant at low temperatures, the RPMD rate constants consistently underestimate the experiment. Since the PES was adjusted to give the best fit to experimental rate constant using the tunneling corrected transition-state theory,(*27*) it is possible that this PES is still not sufficiently accurate. For example, the PES has an imaginary frequency of 1549 cm^{-1} at the transition state, which is significantly smaller than the *ab initio* values of more than 2100 cm^{-1}.(*27*) A thinner barrier might facilitate more facile tunneling.

To summarize, thermal rate constants for an important combustion reaction have been computed using the RPMD method over a large temperature range. The agreement with experimental results is reasonably good. In particular, it reproduces the curvature in the temperature dependence of the rate constant at low temperatures, due apparently to tunneling. The agreement with previous MCTDH results on the same PES is quite impressive, but may be fictitious. On the other hand, the variational transition-state theory with semi-classical tunneling corrections seems to overestimate the rate constants, presumably due to barrier recrossing and inaccurate description of tunneling. Perhaps most importantly, it is shown that only a small number of beads in the RPMD simulations is sufficient to capture the quantum effects in reactions involving the transfer of a light atoms, suggesting RPMD calculations are feasible on much larger systems.

Acknowledgements: YL, HG, and WHG were supported by the Department of Energy (DE-FG02-05ER15694 to HG and DE-FG02-98ER14914 to WHG). YVS acknowledges the support

of a Combustion Energy Research Fellowship through the Combustion Energy Frontier Research Center, an Energy Frontier Research Center funded by the U.S. Department of Energy, Office of Basic Energy Sciences under Award Number DE-SC0001198. MY acknowledges funding from National Science Foundation of China (Projects No. 21073229 and 20833007). HG thanks Joaquin Espinosa-García, David Manolopoulos and Uwe Manthe for several useful discussions.

References:

1. Barker, J. R., and Golden, D. M. Master equation analysis of pressure-dependent atmospheric reactions, *Chem. Rev.* **2003,** *103*, 4577-4591.
2. Fernandez-Ramos, A., Miller, J. A., Klippenstein, S. J., and Truhlar, D. G. Modeling the kinetics of bimolecular reactions, *Chem. Rev.* **2006,** *106*, 4518-4584.
3. Baulch, D. L., Bowman, C. T., Cobos, C. J., Cox, R. A., Just, T., Kerr, J. A., Pilling, M. J., Stocker, D., Troe, J., Tsang, W., Walker, R. W., and Warnatz, J. Evaluated kinetic data for combustion modeling: Supplement II, *J. Phys. Chem. Ref. Data* **2005,** *34*, 757.
4. Althorpe, S. C., and Clary, D. C. Quantum scattering calculations on chemical reactions, *Annu. Rev. Phys. Chem.* **2003,** *54*, 493-529.
5. Guo, H. Quantum dynamics of complex-forming bimolecular reactions, *Int. Rev. Phys. Chem.* **2012,** *31*, 1-68.
6. Manthe, U. Accurate calculations of reaction rates: predictive theory based on a rigorous quantum transition state concept, *Mole. Phys.* **2011,** *109*, 1415-1426.
7. Truhlar, D. G., Issacson, A. D., and Garrett, B. C. (1985) Generalized Transition State Theory, In *Theory of Chemical Reaction Dynamics* (Bear, M., Ed.), pp 65-137, CRC, Boca Raton.
8. Nguyen, T. L., Stanton, J. F., and Barker, J. R. A practical implementation of semi-classical transition state theory for polyatomics, *Chem. Phys. Lett.* **2010,** *499*, 9-15.
9. Miller, W. H. Semi-classical theory for non-separable systems:. Construction of “good” action-angle variables for reaction rate constants, *Faraday Disc. Chem. Soc.* **1977,** *62*, 40–46.
10. Miller, W. H., Hernandez, R., Handy, N. C., Jayatilaka, D., and Willetts, A. Ab initio calculation of anharmonic constants for a transition state, with application to semiclassical transition state tunneling probabilities, *Chem. Phys. Lett.* **1990,** *172*, 62-68.
11. Craig, I. R., and Manolopoulos, D. E. Quantum statistics and classical mechanics: Real time correlation frunction from ring polymer molecular dynamics, *J. Chem. Phys.* **2004,** *121*, 3368-3373.
12. Chandler, D., and Wolynes, P. G. Exploiting the isomorphism between quantum theory and classical statistical mechanics of polyatomic fluids, *J. Chem. Phys.* **1981,** *74*, 4078-4095.
13. Craig, I. R., and Manolopoulos, D. E. Chemical reaction rates from ring polymer molecular dynamics, *J. Chem. Phys.* **2005,** *122*, 084106.
14. Craig, I. R., and Manolopoulos, D. E. A refined ring polymer molecular dynamics theory of chemical reaction rates, *J. Chem. Phys.* **2005,** *123*, 034102.
15. Bennett, C. H. (1977) Molecular dynamics and transition state theory: the simulation of infrequent events, In *Algorithms for Chemical Computations, ACS Symposium Series* (Christofferson, R. E., Ed.), ACS.
16. Chandler, D. Statistical mechanics of isomerization dynamics in liquids and the transition state approximation, *J. Chem. Phys.* **1978,** *68*, 2959-2970.
17. Collepardo-Guevara, R., Suleimanov, Y. V., and Manolopoulos, D. E. Bimolecular reaction rates from ring polymer molecular dynamics, *J. Chem. Phys.* **2009,** *130*, 174713.
18. Suleimanov, Y. V., Collepardo-Guevara, R., and Manolopoulos, D. E. Bimolecular reaction rates from ring polymer molecular dynamics: Application to H + CH_4 --> H_2 + CH_3, *J. Chem. Phys.* **2011,** *134*, 044131.
19. Kästner, J., and Thiel, W. Bridging the gas between thermodynamic integration and umbrella sampling provides a novel analysis method: "umbrella integration", *J. Chem. Phys.* **2005,** *123*, 144104.

20. Corchado, J. C., Espinosa-García, J., Roberto-Neto, O., Chuang, Y.-Y., and Truhlar, D. G. Dual-level direct dynamics calculations of the reaction rates for a Jahn-Teller reaction: Hydrogen abstraction from CH_4 or CD_4 by $O(^3P)$, *J. Phys. Chem. A* **1998,** *102*, 4899-4910.
21. González, M., Hernando, J., Millán, J., and Sayós, R. Ab initio ground potential energy surface, VTST and QCT study of the $O(^3P)+CH_4(X\,^1A_1)\rightarrow OH(X\,^2\Pi)+CH_3(X\,^2A_2'')$ reaction, *J. Chem. Phys.* **1999,** *110*, 7326-7338.
22. Perez de Tudela, R., Aoiz, F. J., Suleimanov, Y. V., and Manolopoulos, D. E. Chemical reaction rates from ring polymer molecular dynamics: Zero point energy conservation in Mu + H_2 --> MuH + H, *J. Phys. Chem. Lett.* **2012,** *3*, 493-497.
23. Stecher, T., and Althorpe, S. C. Improved free energy interpolation scheme for obtaining gas phase reaction rates from ring polymer molecular dynamics, *Mole. Phys.* **2012,** *110*, 875-883.
24. Richardson, J. O., and Althorpe, S. C. Ring-polymer molecular dynamics rate-theory in the deep-tunneling regime: Connection with semi-classical instanton theory, *J. Chem. Phys.* **2009,** *131*, 214106.
25. Gardiner, W. C. *Combustion Chemistry*, Springer, Berlin, 1984.
26. Truhlar, D. G., and Gordon, M. S. From force fields to dynamics: Classical and quantal paths, *Science* **1990,** *249*, 491-498.
27. Espinosa-García, J., and García-Bernáldez, J. C. Analytical potential energy surface for the CH_4 + $O(^3P)$ --> CH_3 + OH reaction. Thermal rate constants and kinetic isotope effects, *Phys. Chem. Chem. Phys.* **2000,** *2*, 2345-2351.
28. Czakó, G., and Bowman, J. M. Dynamics of the $O(^3P)$ + $CHD_3(v_{CH}=0,1)$ reactions on an accurate ab initio potential energy surface, *Proc. Natl. Acad. Sci. USA* **2012,** *109*, 7997-8001.
29. Troya, D., and García-Molina, E. Quasiclassical trajectory study of the $O(^3P)$ + CH_4 --> OH + CH_3 reaction with a specific reaction parameters semiempirical Hamiltonian, *J. Phys. Chem. A* **2005,** *109*, 3015-3023.
30. Varandas, A. J. C., Caridade, P. J. S. B., Zhang, J. Z. H., Cui, Q., and Han, K. L. Dynamics of X+CH_4 (X = H,O,Cl) reactions: How reliable is transition state theory for fine-tuning potential energy surfaces?, *J. Chem. Phys.* **2006,** *125*, 064312.
31. Clary, D. C. Quantum dynamics of the $O(^3P)$ + CH_4 --> OH + CH_3 reaction, *Phys. Chem. Chem. Phys.* **1999,** *1*, 1173-1179.
32. Yu, H.-G., and Nyman, G. Quantum dynamics of the $O(^3P)$ + CH_4 --> OH + CH_3 reaction: An application of the rotating bond umbrella model and spectral transform subspace iteration, *J. Chem. Phys.* **2000,** *112*, 238-247.
33. Wang, M.-L., Li, Y.-M., and Zhang, J. Z. H. Application of semirigid vibrating rotor target model to the reaction of $O(^3P)$ + CH_4 --> CH_3 + OH reaction, *J. Phys. Chem. A* **2001,** *105*, 2530-2534.
34. Yang, M., Lee, S.-Y., and Zhang, D. H. Seven-dimensional quantum dynamics study of the $O(^3P)+CH_4$ reaction, *J. Chem. Phys.* **2007,** *126*, 064303.
35. Huarte-Larrañaga, F., and Manthe, U. Accurate quantum dynamics of a combustion reaction: Thermal rate constants of $O(^3P)$ + $CH_4(X^1A_1)$ --> $OH(X^2P)$ + $CH_3(X^2A''_2)$, *J. Chem. Phys.* **2002,** *117*, 4635-4638.
36. Suleimanov, Y. V., Allen, J. W., and Green, W. H. RPMDrate: bimolecular chemical reaction rates from ring polymer molecular dynamics, *Comput. Phys. Comm.* **2012,** *in press* http://dx.doi.org/10.1016/j.cpc.2012.10.017,.
37. Markland, T. E., and Manolopoulos, D. E. An efficient ring polymer contraction scheme for imaginary time path integral simulations, *J. Chem. Phys.* **2008,** *129*, 024105.
38. Cohen, N. A reevaluation of low temperature experimental rate data for the reactions of O atoms with methane, ethane, and neopentane, *Int. J. Chem. Kinet.* **1986,** *18*, 59-82.

Figure captions:

Fig. 1 Potentials of mean force (PMFs) for the title reaction at 600 K with one (dashed line) and eight beads (solid line).

Fig. 2 Convergence of RPMD rate constants with respect to the number of beads.

Fig. 3 Comparison of the rate constants with experimental and previous theoretical results.

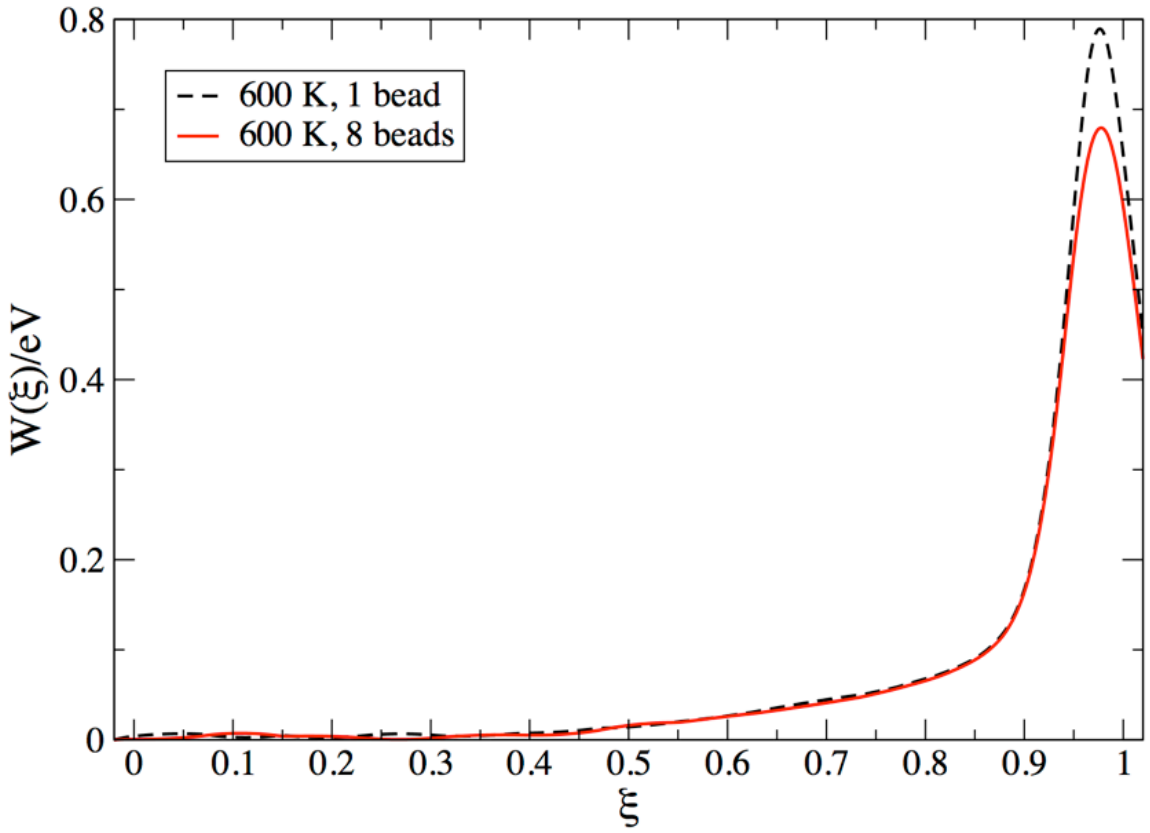
600 K, 1 bead
600 K, 8 beads
W(ξ)/eV
ξ
0
0.2
0.4
0.6
0.8
0
0.1
0.2
0.3
0.4
0.5
0.6
0.7
0.8
0.9
1

Fig. 1

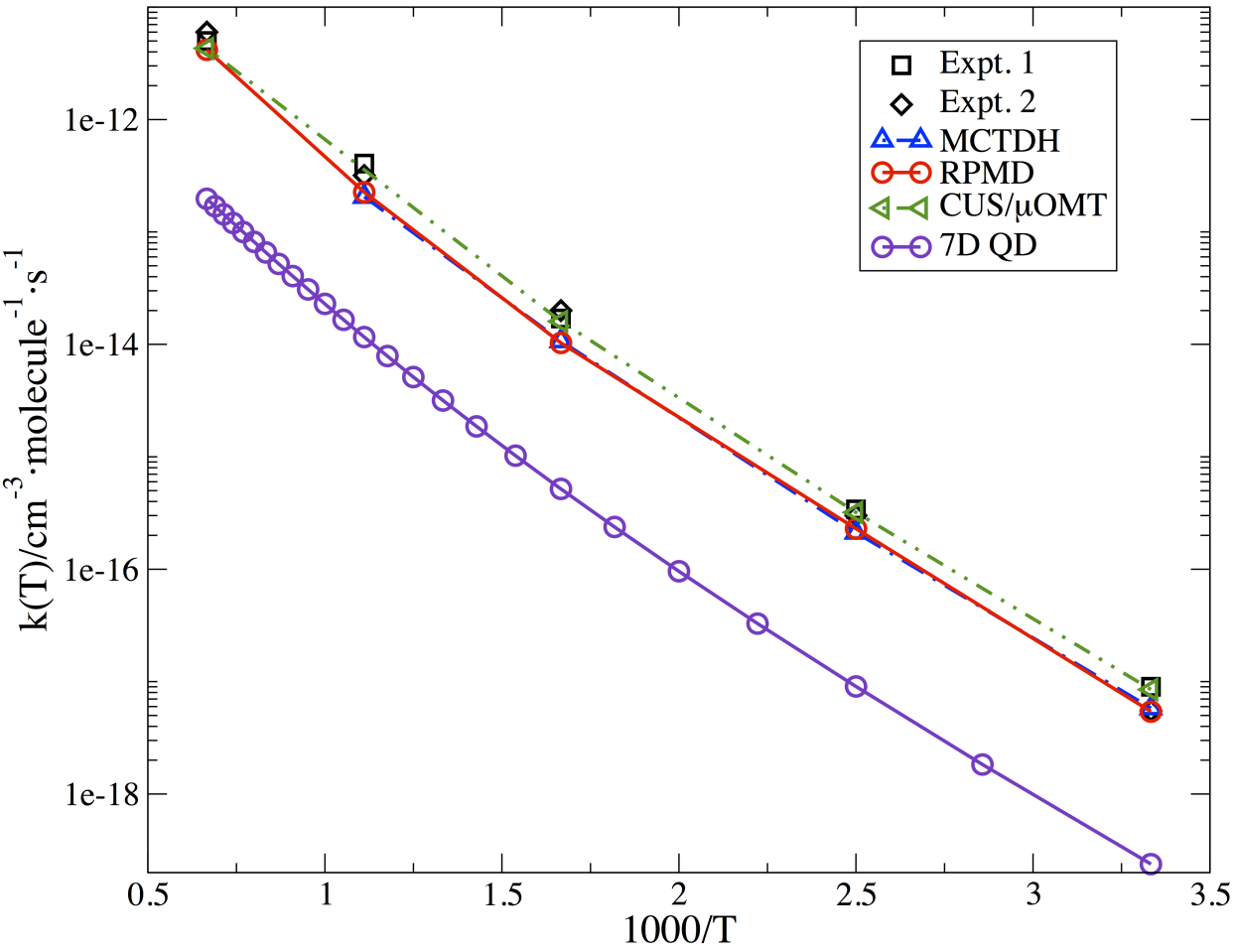
Expt. 1
Expt. 2
MCTDH
RPMD
CUS/μOMT
7D QD
1e-12
1e-14
1e-16
1e-18
k(T)/cm^{-3}·molecule^{-1}·s^{-1}
0.5
1
1.5
2
2.5
3
3.5
1000/T

Fig. 2

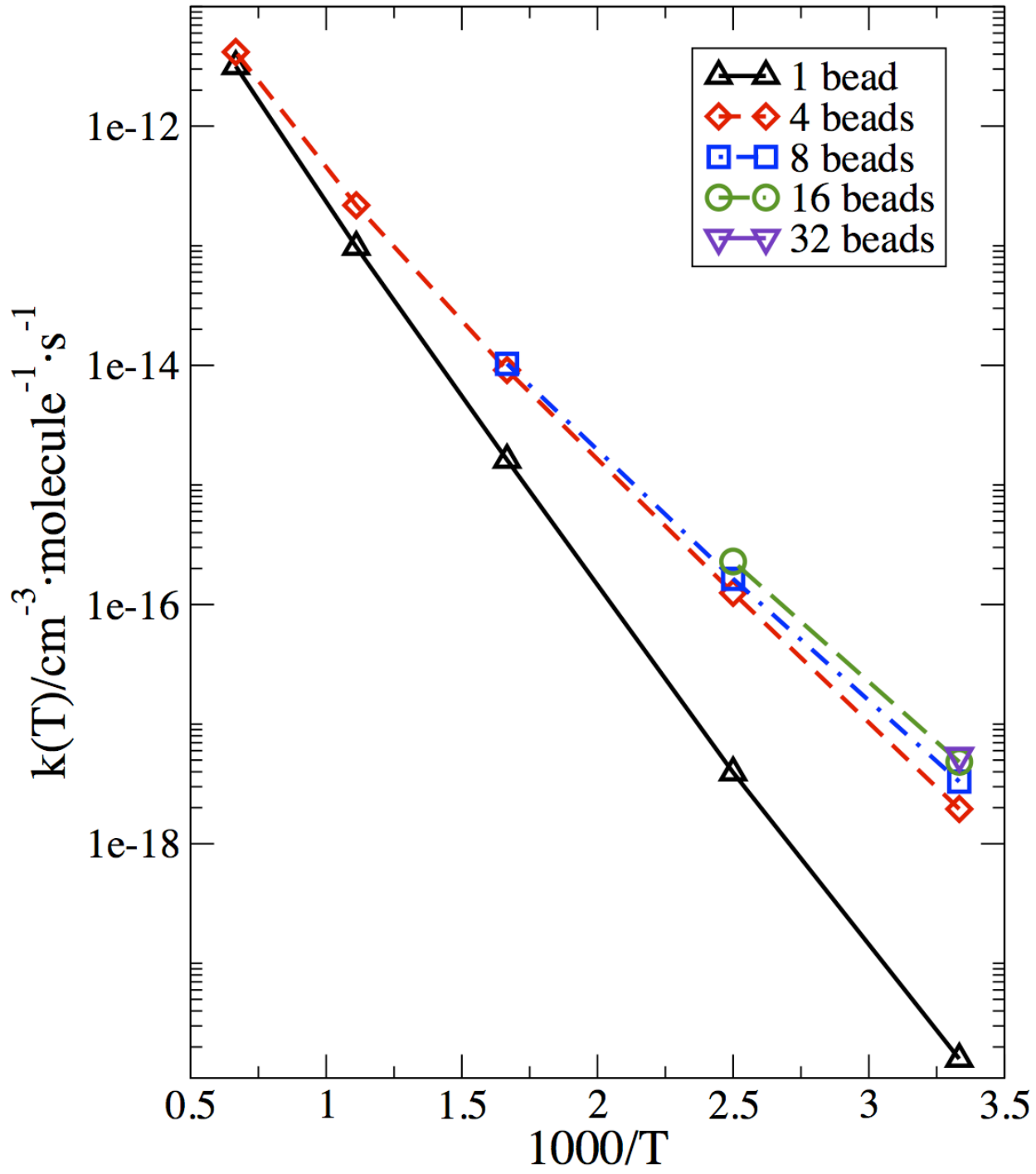
1 bead
4 beads
8 beads
16 beads
32 beads
1e-12
1e-14
1e-16
1e-18
k(T)/cm-3·molecule-1·s-1
0.5
1
1.5
2
2.5
3
3.5
1000/T

Fig. 3

Table. I. Calculated rate constants from RPMD with different temperatures and comparison with both experimental and previous theoretical data.

T(K)	300	400	600	900	1500
N_{bead}	32	16	8	4	4
ΔG(eV)	0.526	0.579	0.679	0.801	0.807
$\xi^{\neq}$	0.984	0.981	0.978	0.976	0.974
k_{QTST}	1.04E-17	4.44E-16	1.98E-14	4.05E-13	8.00E-12
κ	0.584	0.615	0.663	0.719	0.728
k_{RPMD}	5.42E-18	2.29E-16	1.03E-14	2.26E-13	4.17E-12
MCTDH	5.81E-18	2.12E-16	1.07E-14	2.06E-13	--
7D QD	2.38E-19	9.05E-18	5.17E-16	1.16E-14	1.97E-13
CUS/μOMT	8.50E-18	3.20E-16	1.60E-14	--	4.30E-12
Expt. 1*	9.00E-18	3.40E-16	1.70E-14	4.06E-13	5.00E-12
Expt. 2*	5.50E-18	3.00E-16	2.00E-14	3.18E-13	6.00E-12

*: The experimental data were taken from Refs. (*38*) and (*3*).